The predictive value of FDG-PET with 3D-SSP for surgical outcomes in patients with temporal lobe epilepsy

Takuma Higo [1], Hidenori Sugano [1], Madoka Nakajima [1], Kostadin Karagiozov [1], Yasushi Iimura [1], Masaru Suzuki [2], Kiyoshi Sato[2], and Hajime Arai [1]

1 Department of Neurosurgery, Juntendo University

2-1-1 Hongo, Bunkyo-ku, Tokyo, Japan, 113-8421

2 PET/CT Research Center, Juntendo Tokyo Koto Geriatric Medical Center, Juntendo University

3-3-20 Shinsuna, Koto-ku, Tokyo, Japan, 1

Corresponding author:

Takuma Higo M.D.

Department of Neurosurgery, Juntendo University

2-1-1 Hongo, Bunkyo-ku, Tokyo 113-8421, Japan

E-mail: thigo@jutendo.ac.jp

Telephone: +81-3-3813-3111

Fax: +81-3-5689-8343

Running title: FDG-PET efficacy for the diagnosis of temporal lobe epilepsy

Abbreviations in this manuscript

FDG-PET: ^{18}F-2-fluorodeoxy-D-glucose positron emission tomography

mTLE: mesial temporal lobe epilepsy

3D-SSP: three-dimensional stereotactic surface projection

HS: hippocampal sclerosis

SAH: selective amygdalohippocampectomy

ATL: anterior temporal lobectomy

RHD: ratio of hypometabolic difference

Abstract

Purpose:

We retrospectively evaluated the diagnostic value of ^{18}F-2-fluorodeoxy-D-glucose positron emission tomography (FDG-PET) with statistical analysis for the foci detection and predictive utility for postsurgical seizure outcome of patients with mesial temporal lobe epilepsy (mTLE).

Method:

We evaluated 40 patients who were diagnosed mTLE and underwent selective amygdalohippocampectomy (SAH) or anterior temporal lobectomy (ATL) in our institute. Preoperative interictal FDG-PET with statistical analysis using three-dimensional stereotactic surface projection (3D-SSP) was detected with several clinical data including seizure semiology, MRI, scalp electroencephalography, surgical procedure with SAH or ATL and postsurgical outcome. The region of interest (ROI) was defined on 'Hippocampus & Amygdala', 'Parahippocampal gyrus & Uncus', 'T1 & T2', and 'T3 & Fusiform gyrus.' We obtained the ratio of hypometabolism difference (RHD) by 3D-SSP, and evaluated the relation among hypometabolic extent, surgical outcome and surgical procedure.

Result:

The RHD in each ROIs ipsilateral to operative side was significantly higher than that of contralateral side in good outcome group. Hypometabolism of 'Hippocampus & Amygdala' was most reliable prognostic factor. Patients of discordant with presurgical examinations hardly showed obvious lateralized hypometabolism. Nevertheless, when

they have significantly high RHD in mesial temporal lobe, good surgical outcome was expected. There was not significant difference of RHD distribution between SAH and ATL in good outcome group.

Conclusion:

Significant hypometabolism in mesial temporal lobe on FDG-PET with 3D-SSP is useful to predict good surgical outcome for patients with mTLE, particularly in discordant patients with hypometabolism in mesial temporal structure. However, FDG-PET is not indicative of surgical procedure.

Highlights

- Hypometabolism was compared among patients with mTLE by concordance and outcome.
- FDG-PET with 3D-SSP can facilitate the prediction of epileptic focus location.
- Hypometabolism in mesial temporal indicated good outcome even in discordant.
- Lateral temporal lobe was debatable for detection with FDG-PET.

1 Introduction

The conventional diagnosis of an epileptic focus location is based on seizure semiology, electroencephalography (EEG), and magnetic resonance imaging (MRI). ^{18}F-2-fluorodeoxy-D-glucose positron emission tomography (FDG-PET) can provide additional information to determine the focus localization by representing foci as hypometabolic areas of glucose (Carne et al., 2004; Kumar et al., 2010; Willmann et al., 2007). Visual assessment of FDG-PET images has been routinely used for clinical evaluation. However, its interpretation is subjective and depends on observer's experience (Drzezga et al., 1999). Hypometabolic areas tend to extend further than actual epileptic foci (Vinton et al., 2007), and often patients with mesial temporal lobe epilepsy (mTLE) show hypometabolic areas spreading across extratemporal or contralateral to the epileptic area.

Recently, objective statistical approaches have been proposed to improve the diagnostic accuracy of epileptic focus localization (Ohta et al., 2008; Soma et al., 2012). They evaluate focus lateralization by an asymmetry index of a specific region of interest (ROI). Z-score mapping that is indicating differences between normal and actual value for each voxel with an asymmetry index using statistical parametric mapping (SPM) improved regional glucose hypometabolism detection (Soma et al. 2011).

In this study, we investigated the diagnostic value of FDG-PET with a three-dimensional stereotactic surface projection (3D-SSP) as a statistical method for patients with TLE. We evaluated the following: 1) Comparison of the diagnostic value of FDG-PET with 3D-SSP to visual inspection for focus detection during pre-operative

diagnostic work-up. 2) Detection of a diagnostically significant region leading to good surgical outcome after using 3D-SSP. 3) Evaluation of differences in FDG-PET findings between patients with or without concordant data from non-invasive presurgical studies. 4) Evaluation of the potential contribution of FDG-PET findings to decide the extent of surgical resection for patients with TLE (selective amygdalohippocampectomy (SAH) vs. anterior temporal lobe resection (ATL)).

2 Materials and methods

Patients with pathologically proven hippocampal sclerosis (HS) who presented at our facility from 2006 to 2013 with complex partial seizures (CPS) that were presumed to originate from the temporal lobe were enrolled in this study. Pre-surgical evaluations of seizure semiology, MRI, scalp video EEG and neuropsychological examinations were performed in all patients. Patients who had a typical CPS and a unilateral HS on MRI with ipsilateral ictal and interictal epileptic discharges (IEDs) from ipsilateral temporal leads on a scalp video EEG belonged to the concordant group. Having concordant data satisfied our indications for an epileptic focus resection without invasive EEG recordings. When the findings were discordant (discordant group), we implanted bilaterally subdural electrodes over the mesial and lateral temporal lobes to record habitual seizures and epileptic discharge patterns for several days (Shimizu et al., 1992).

We performed a trans-sylvian selective amygdalohippocampectomy (SAH) with recording of intraoperative electrocorticography (ECoG) from the hippocampus,

amygdala and lateral temporal cortex under 2.5% sevoflurane anaesthesia (Inoue et al., 2000). After resecting the mesial temporal lobe structures, we again recorded the ECoG from the lateral temporal cortex. When some persisting epileptic discharges were recorded from the lateral temporal lobe, we carried out an additional lateral temporal resection.

The postsurgical seizure outcomes were evaluated using the classification of the international league against epilepsy (ILAE) committee (Wieser et al., 2001) at 1-year and 2-years after surgery. Class 1 and 2 ILAE classifications were regarded as good surgical outcomes, and class 3 to 6 were considered to be poor.

Data acquisition for the ^{18}F-FDG-PET with 3D-SSP analysis

The ^{18}F-FDG PET scans were performed using a Discovery ST scanner (General Electric Healthcare, Fairfield, Connecticut, USA). The trans-axial spatial resolutions (full width at half maximum) at 1- and 10-cm off-axes were 6.2 and 6.7 mm, respectively. The subjects fasted for at least 4 hours before the scan. After an intravenous administration of 185 MBq/2 ml ^{18}F-FDG, the subjects were kept in a dimly illuminated isolation room and instructed to remain still with their eyes open and to avoid falling asleep. A set of trans-axial images was obtained in a standard 3D emission scan mode starting 40 minutes after the injection with scan duration of 15 min. The images were reconstructed using 3-dimensional iterative reconstruction, including a correction for attenuation measured by a transmission scan. The matrix size, each voxel size, slice thickness, and number of images were 128×128 mm, 2.25 mm, 3.3 mm, and

47 slices, respectively.

We analysed the FDG-PET images using 3D-SSP in NEUROSTAT developed by Minoshima (Minoshima et al., 1992; Minoshima et al., 1995; Minoshima et al., 1994), in which the cerebral metabolic rate of glucose (CMRglc) was projected over a standardized anatomical brain. For anatomic standardization, first, the midsagittal plane of the brain is determined from the PET image set, and the bicommisural anterior commissure to posterior commissure (AC-PC) line is defined on the midsagittal plane. In this way, the AC-PC line is matched to the center of the co-ordinate system of the atlas's brain. Next, individual brain size is corrected linearly to the standard dimension of the atlas brain. The anteroposterior length was measured as the distance between the most anterior edge of frontal cortex and the most posterior edge of the occipital cortex. The brain width was measured as the distance between the midsagittal plane and the most lateral edge of the parietotemporal cortex. The brain height was measured by matching midsagittal plane derived and fitted to the brain contour in the atlas varying the vertical scale linearly.

To extract metabolic data after anatomic standardization for cortical metabolic activity, pixels located on the outer and medial surface of both hemispheres are predetermined along with three-dimensional vectors perpendicular to the surface at each pixel. For each predetermined pixel, the techniques each for the highest pixel value in a direction inward along the vector to a six-pixel depth (13.5 mm) into the cortex on the individual's anatomically standardized PET image set and assigned the maximum value to the surface pixel.

The CMRglc images were normalized to the mean whole brain CMRglc activity. A normal database was acquired from 26 Japanese volunteers (13 males and 13 females) ranging from 40- to 64-year-olds from the Juntendo Tokyo Koto geriatric medical centre-using the same PET scanning technique (Iseki et al., 2010). The number of volunteer under 50 years old was 10 (5 male, 5 female. average 44.2 yeas old), 50 to 60 was 10 (6 male, 4 female. average 54.5 years old), and 61 to 64 was 5 (2 male, 4 female. Average 61.8 years old). The 3D-SSP was performed using normal data with the decade of age matched. When a patient's age was below 40, we used the data from the 40-year decade as the normal. The region of interests (ROIs) to evaluate the CMRglc in this study were the following: "Hippocampus & Amygdala", "Parahippocampal & Uncus", "T1 & T2 gyri", and "T3 & Fusiform gyri". Individual anatomical information was converted to standardized brain mapping using the Talairach Daemon brain atlas. The template of standardized brain was obtained by Talairach Client 2.4 program(Lancaster, 2000). To demonstrate the regional patterns of CMRglc, a two-sample *t*-test was performed to obtain Z-scores on a voxel-by-voxel basis between each patient and the normal database using the stereotactic extraction estimation (Koutroumanidis et al.) program developed by Mizumura *et al.* (Mizumura and Kumita, 2006). The 1.96 value of the Z-scores was automatically defined and values less than 1.96 were rejected by definition. To illustrate the extent of hypometabolism in each ROI, we defined the ratio of hypometabolism difference (RHD) in each ROI by dividing the number of voxels established for each patient by the number of voxels as a control.

Comparing the 3D-SSP and Visual analysis of FDG-PET

To evaluate the 3D-SSP method in relation to the existing conventional approach, we compared the two methods. On visual assessment, the FDG-PET images were evaluated by an expert neurosurgeon and a neuroradiologist who were blinded for the patients' background and surgical results. The decision was only for the existence of laterality within the temporal lobe, not the localization or extent of the hypometabolic area. If it was difficult to decide on certain case, it was considered to be 'unknown'. When the two examiners had different decisions, the case was also considered to be "unknown". Cohen's kappa score was 0.75, which was regarded as a good agreement.

Evaluation of the diagnostic value of 3D-SSP

We evaluated the potential diagnostic value of the 3D-SSP (RHD) by validating it in the good outcome group. We compared the following: 1) *The significance of RHD values to predict good surgical outcome and identify correctly epileptic focus location.* Subsequently, we established a statistically significant threshold of RHD in the positive ROI using a receiver operating characteristics (ROC) curve. 2) *The differences in RHD values between the concordant and discordant groups.* Within the discordant group, we tried to find a benefit from 3D-SSP application to predict good surgical candidates before surgery. We compared the RHD values in ROIs to surgical outcome. 3) *The assessment of RHD for choosing the extent of surgical resection,* SAH or ATL, contributing to the adequacy of resection extent. From both surgical procedures, we re-selected the 3D-SSP data for those patients with good

surgical outcome. Analysis of the RHD distributions between the SAH and ATL groups was performed.

Statistical analysis

All statistical analyses were performed with IBM SPSS version 22 software (IBM Corp., Armonk, NY, USA). The comparison between the visual and 3D-SSP statistical analyses was performed using a chi-square test. To examine which ROI contributed to a good surgical outcome, multiple logistic regressions test were performed. The differences of the RHD distributions on the ROI between "the concordant and discordant groups" and "SAH and ATL groups" were evaluated by a Wilcoxon rank test. A *p*-values less than 0.05 were considered statistically significant in all of the analyses in this study.

3 Results

Comparison between 3D-SSP and Visual analysis of FDG-PET

Forty surgically treated patients (18 males, 22 females, with average age 32.1 years, range 11-63 years) were registered to evaluate the significance of FDG-PET with statistical analysis. There were 26 and 14 patients in the concordant and discordant groups, respectively.

Examples of MRI and FDG-PET images with or without 3D-SSP are presented in figure 1. In the concordant group, 21 patients (80.8%) were detected with obvious ipsilateral hypometabolism by visual inspection. On the other hand, in the

discordant group, only two patients (14.3%) had ipsilateral hypometabolism detected by the expert observers. After the 3D-SSP, the positive finding for laterality did not increase in the concordant group, and two additional patients with right HS could be detected in the discordant group. These data however were not statistically significant.

Postsurgical outcome 1-year after surgery revealed that 30 patients (75%) resulted in good surgical outcome. Twenty-three of the 26 patients in the concordant group had good outcomes (88.5%). However, only 7 of the 14 patients (50.0%) in the discordant group had good outcomes. At 2-years after surgery, postsurgical outcome of all patients was kept the same as 1-year outcome.

We compared the surgical outcome and hypometabolism comparing between patients with right and left mTLE. We had 25 patients (good: 18, poor: 7) with right mTLE and 15 patients (good: 12, poor: 3) with left mTLE. The ratio of good outcome was 72% and 80%, respectively. There was no statistical difference. The value of RHD in each ROI between two groups was also compared. There was not significant difference in any ROI.

We investigated the hypometabolism in extratemporal regions including frontal lobe, parietal lobe, occipital lobe and thalamus. However, none of them had significant RHD with 3D-SSP detection. We did not find any relation between the extratemporal hypometabolism and postsurgical outcome.

Patients were also divided into younger and elder group to compare temporal hypometabolism, concordance, and outcome by a generation. The median age of them was 29.5 years old, and they were grouped into under 30-years-old and more than or

equal 30-years-old. The younger group consist of 20 patients (10 male and 10 female). Twelve patients were in concordant group and 8 were in discordant group. Sixteen patients resulted in good outcome. The elder group was composed of 20 patients (8 male and 12 female). Twelve patients were in concordant group, and 14 patients resulted in good outcome. Chi-test was performed but there was no statistically difference of postsurgical outcome or concordance between two groups.

RHD in each ROI between two group was compared by Student t-test, and RHD 'Hippocampus & Amygdala' and 'Parahippocampal & Uncus' showed significantly higher value in younger group (p=0.002 and 0.04, respectively).

Significance of the RHD value differences to predict good surgical outcome

In the good surgical outcome group, the RHD on the ipsilateral side was significantly higher than that of the contralateral side. Multiple logistic regressions to identify which regions were predictive for a good surgical outcome showed that the RHD of 'Hippocampus & Amygdala' was the most significant (p =0.025) (Figure 2).

ROC analysis was also performed to evaluate the RHD of 'Hippocampus & Amygdala' as a predictor of postsurgical outcome. ROC curve of RHD of 'Hippocampus & Amygdala' was described and area under the curve (AUC) was 0.755 with standard error = 0.017 and 95% confidence interval from 0.561 to 0.949. According to the ROC curve, the best cut-off value with maximum sensitivity (0.7) and minimum fall-out (0.3) was 0.22. We concluded that patients with RHD above 22% were expected to have good surgical outcome (Figure 3).

Differences in RHD characteristics between the concordant and discordant groups

The comparison of RHD averages between the concordant and discordant groups for all of the ROIs is presented in Figure 4. In both groups, the same characteristic RHD distributions were detected. However, the value of RHD in the "Hippocampus & Amygdala" ROI in the concordant group was significantly higher (mean 44.6%) than that of the discordant group. In the discordant group, the differences of RHD distribution showed that the good outcomes had a higher percentage of RHD in the ipsilateral "Hippocampus & Amygdala" ROI (mean 43.0%) (Figure 5). On the other hand, the patients with poor outcomes had apparently lower RHDs in all of the ROIs and no difference with the contralateral side. In this way, we found that four of the 14 patients were good surgical candidates according to the 3D-SSP results (28.6%).

Assessment of RHD for deciding the extent of surgical resection (SAH or ATL)

Seventeen of the 26 patients in the concordant group underwent a SAH. Fourteen had good outcome. All nine patients in the ATL group had good outcome, too. In the discordant group, three of the 14 patients underwent SAH, and had good outcome, and 11 patients received ATL and six had good outcome. In total, we performed SAH in 20 patients and ATL in 20 patients.

There was no obvious difference in the extent of hypometabolism between the groups of different surgical technique in respect to the outcome. That made us consider that the RHD values of the lateral temporal areas were not significantly indicative for a

surgical procedure extension from SAH to ATL.

4 Discussion

The value of hypometabolic focus detection as an indicator of the epileptic focus location has been accepted, particularly for decisions on laterality(Carne et al., 2004; Erbayat Altay et al., 2005; Theodore et al., 1997; Vinton et al., 2007). The relation between MRI, FDG-PET findings and surgical outcomes has been extensively discussed (Chassoux et al., 2004; Joo et al., 2005; LoPinto-Khoury et al., 2012; Sakamoto et al., 2009; Takahashi et al., 2012; Wong et al., 2012). Willmann *et al.* performed a meta-analysis and showed that ipsilateral PET hypometabolism had an 86% predictive value of a good surgical outcome. They also reported that the predictive value was 80% in patients with a normal MRI and 72% in patients with a non-localized scalp EEG(Willmann et al., 2007). FDG-PET also shows hypometabolism in the lateral temporal and to some degree the extra-temporal regions even in patients with mesial TLE (Kim et al., 2003). However, the meaning of these positive findings is still unknown. Therefore, in this study we strictly selected patients with HS manifesting with CPS and tried to determine the value of hypometabolism also in the extra-mesial temporal lobe. In addition, we considered the value of the data from FDG-PET with statistical analysis to improve surgical outcomes for patients with mTLE.

Visual analysis of FDG-PET has the deficiency of subjectivity, although many research groups indicate a high or absolute degree of inter-observer agreement. Although we accept the high degree of inter-observer agreement, the development of an

objective and quantitative FDG-PET approach requires standardizing a normal value of metabolism. Several statistical approaches for evaluating FDG-PET have applied SPM and we used 3D-SSP in this study because we already had a reliable normal database (Iseki et al., 2010). A limitation for our method was that we indicated normal values of CMRglu from healthy normal volunteers who had higher average age than that of our patients' group, as we know that it gradually decreases with age (Knopman, 2014). Therefore, our RHD values in younger patients should result from lower CMRglu in general because it is ethically difficult to establish the normal database consist of childhood or adolescent volunteers. The evaluation of younger patients with elder normal database become severe, although hypometabolism might be overestimated. A normal database with completely age matched CMRglu from the same PET scanner would be ideal for evaluation. Both SPM and 3D-SSP have similar algorithms for evaluating the CMRglu of each patient voxel by voxel after a 3D integration with the Talairach`s atlas. The merit of the 3D-SSP was the application of SEE software to perform quantitative evaluation in each ROI. The patients in the concordant group did not show any advantage in using the 3D-SSP for detecting focus laterality, just validating the method against the available standards. While the 3D-SSP detected two additional patients in the discordant group, that was not a statistically significant contribution. However, we found consistently a localization of low CMRglu in the "Hippocampus & Amygdala" ROIs using the 3D-SSP. It is believed that pathological, concomitant with metabolic changes in the temporal pole exist in patients with mTLE(Najm et al., 2006; Rubin et al., 1995; Semah et al., 1995). Because the 3D-SSP

with SEE does not specifically define the temporal pole as ROI, we evaluated the 3D-SSP mapping by visual inspection and consequently positive Z-score mapping did not appear in the temporal pole through our analysis.

Significant hypometabolism in the mesial temporal lobe on the FDG-PET with 3D-SSP is indicative of good outcomes, even in patients without a concordance of presurgical examinations in our study. Previous reports also mentioned that temporal hypometabolism of the mesial temporal lobe was a better predictor for seizure control than lateral temporal hypometabolism (Delbeke et al., 1996). The patients of the poor surgical outcome group tended to have a lower RHD throughout all of the ROIs. We established that the threshold of significance as a cut-off value from the RHD of the "Hippocampus & Amygdala" was 22% in our method. According to this value, the region with more than a 22% volume of significant hypometabolism is indicative of an epileptogenic zone in practical terms. Resection of such area can yield good outcomes. The other regions of less than 22% of the RHD were having less predictive value for focus detection. However, the 22% cut-off value is only useful in our facility. Examiners should calculate their own cut-off values from their individual normal databases and outcomes. Broad area or extratemporal hypometabolism is associated with residual postsurgical seizure activity in patients with TLE (Wong et al., 2010). However, we did not have any patients who showed higher RHD values in wide areas, probably because we selected patients only with HS pathology. When we expand the subjects without HS, the extent of the hypometabolic area could be a predictive factor to detect a precise focus, and surgical outcomes will be supposed to be similar to previous

reports (Hajek et al., 1993). Even in that situation, an established cut-off value of the RHD could be useful to select patients and obtain good outcomes.

The patients who showed an obvious laterality on presurgical examinations also expressed significant hypometabolism in the ipsilateral hippocampus and amygdala at the surgical side. Therefore, we also explored the role of the 3D-SSP in the discordant group to explore for the same relation. The patients who did not have significantly higher RHDs did not benefit from surgery. Although some authors indicated that the FDG-PET was the most valuable decision-making examination for surgical treatment in patients who showed discordant data, the important factor to indicate surgery was a higher value of RHD in the specific areas, such as the hippocampus and amygdala.(Uijl et al., 2007; Wong et al., 2012). Because the surgical decision was taken on the basis of the intracranial EEG in the discordant group, it can be supposed that the FDG-PET with 3D-SSP could become complementary to an invasive electrode recording within the diagnostic algorithm.

There is still controversy regarding the ability of FDG-PET to indicate the need for extending resection areas (from SAH to ATL). Our protocol used the intraoperative ECoG to decide if additional resection of the lateral temporal lobe was needed. Our RHD data at the lateral temporal lobe did not show a significant relation to the residual epileptic activity on the intraoperative ECoG. Similar to our results, Parker *et al.* concluded that FDG-PET had no value in the decision to extend the resection in temporal lobe surgery (Parker and Levesque, 1999). However, Liew et al. mentioned the existence of hypometabolism in the lateral temporal lobe in patients with a mTLE and

extension of pathological changes laterally (Liew et al., 2009). Because we strictly selected patients with HS in this study, we did not have pathological changes in the lateral temporal structures. Therefore, our RHD data at the lateral temporal did not reflect clearly the existence of pathological changes. Nevertheless, the RHDs of the lateral temporal in the patients with good outcome were relatively higher, although not significant, than those in patients with poor outcome. Some relations in the mesial temporal structures to the lateral cortex should be considered, such as structural differences and connectivity as a possible reason for these observations. We still have to investigate the glucose metabolic relations between the mesial temporal lobe to surrounding areas.

Conclusion

FDG-PET with statistical analysis using the 3D-SSP was able to provide an automatic quantitative expression of hypometabolism in ROIs. Higher RHDs in the hippocampus and amygdala positively predicted surgical outcomes in patients with the concordant, but also with discordant data from presurgical non-invasive studies. The RHDs at the lateral temporal lobe did not clearly indicate the need of lateral temporal lobe resection. The RHDs at the lateral temporal lobe of the epileptogenic side did not show concordance with intra-operative ECoG.

References

Carne, R.P., O'Brien, T.J., Kilpatrick, C.J., MacGregor, L.R., Hicks, R.J., Murphy, M.A., Bowden, S.C., Kaye, A.H., Cook, M.J., 2004. MRI-negative PET-positive temporal lobe epilepsy: a distinct surgically remediable syndrome. Brain : a journal of neurology 127, 2276-2285.

Chassoux, F., Semah, F., Bouilleret, V., Landre, E., Devaux, B., Turak, B., Nataf, F., Roux, F.X., 2004. Metabolic changes and electro-clinical patterns in mesio-temporal lobe epilepsy: a correlative study. Brain : a journal of neurology 127, 164-174.

Delbeke, D., Lawrence, S.K., Abou-Khalil, B.W., Blumenkopf, B., Kessler, R.M., 1996. Postsurgical outcome of patients with uncontrolled complex partial seizures and temporal lobe hypometabolism on 18FDG-positron emission tomography. Investigative radiology 31, 261-266.

Drzezga, A., Arnold, S., Minoshima, S., Noachtar, S., Szecsi, J., Winkler, P., Romer, W., Tatsch, K., Weber, W., Bartenstein, P., 1999. 18F-FDG PET studies in patients with extratemporal and temporal epilepsy: evaluation of an observer-independent analysis. Journal of nuclear medicine : official publication, Society of Nuclear Medicine 40, 737-746.

Erbayat Altay, E., Fessler, A.J., Gallagher, M., Attarian, H.P., Dehdashti, F., Vahle, V.J., Ojemann, J., Dowling, J.L., Gilliam, F.G., 2005. Correlation of severity of FDG-PET hypometabolism and interictal regional delta slowing in temporal lobe epilepsy. Epilepsia 46, 573-576.

Hajek, M., Antonini, A., Leenders, K.L., Wieser, H.G., 1993. Mesiobasal versus lateral temporal lobe epilepsy: metabolic differences in the temporal lobe shown by interictal 18F-FDG positron emission tomography. Neurology 43, 79-86.

Inoue, S., Hayashi, K., Shigemi, K., Tanaka, Y., 2000. [An anesthetic experience of epileptic focus resection in a nine month-old girl under monitoring by

electrocorticography]. Masui. The Japanese journal of anesthesiology 49, 667-670.

Iseki, E., Murayama, N., Yamamoto, R., Fujishiro, H., Suzuki, M., Kawano, M., Miki, S., Sato, K., 2010. Construction of a (18)F-FDG PET normative database of Japanese healthy elderly subjects and its application to demented and mild cognitive impairment patients. International journal of geriatric psychiatry 25, 352-361.

Joo, E.Y., Hong, S.B., Han, H.J., Tae, W.S., Kim, J.H., Han, S.J., Seo, D.W., Lee, K.H., Hong, S.C., Lee, M., Kim, S., Kim, B.T., 2005. Postoperative alteration of cerebral glucose metabolism in mesial temporal lobe epilepsy. Brain : a journal of neurology 128, 1802-1810.

Kim, Y.K., Lee, D.S., Lee, S.K., Kim, S.K., Chung, C.K., Chang, K.H., Choi, K.Y., Chung, J.K., Lee, M.C., 2003. Differential features of metabolic abnormalities between medial and lateral temporal lobe epilepsy: quantitative analysis of (18)F-FDG PET using SPM. Journal of nuclear medicine : official publication, Society of Nuclear Medicine 44, 1006-1012.

Knopman, D. S.Jack, C. R., Jr.Wiste, H. J.Lundt, E. S.Weigand, S. D.Vemuri, P. Lowe, V. J.Kantarci, K.Gunter, J. L.Senjem, M. L.Mielke, M. M.Roberts, R. O. Boeve, B. F.Petersen, R. C., 2014. 18F-fluorodeoxyglucose positron emission tomography, aging, and apolipoprotein E genotype in cognitively normal persons. Neurobiology of aging 35, 2096-2106.

Koutroumanidis, M., Binnie, C.D., Elwes, R.D., Polkey, C.E., Seed, P., Alarcon, G., Cox, T., Barrington, S., Marsden, P., Maisey, M.N., Panayiotopoulos, C.P., 1998. Interictal regional slow activity in temporal lobe epilepsy correlates with lateral temporal hypometabolism as imaged with 18FDG PET: neurophysiological and metabolic implications. Journal of neurology, neurosurgery, and psychiatry 65, 170-176.

Kumar, A., Juhasz, C., Asano, E., Sood, S., Muzik, O., Chugani, H.T., 2010. Objective detection of epileptic foci by 18F-FDG PET in children undergoing epilepsy surgery. Journal of nuclear medicine : official publication, Society of Nuclear Medicine 51,

1901-1907.

Lancaster, J.L., Woldorff, M.G., Parsons, L.M., Liotti, M., Freitas, C.S., Rainey, L., Kouchunov, P.V., Nickerson, D., Mikiten, S.A., Fox, P.T., 2000. Automated Talairach atlas labels for functional brain mapping. Human Brain Mapping 10, 120-131.

Liew, C.J., Lim, Y.M., Bonwetsch, R., Shamim, S., Sato, S., Reeves-Tyer, P., Herscovitch, P., Dustin, I., Bagic, A., Giovacchini, G., Theodore, W.H., 2009. 18F-FCWAY and 18F-FDG PET in MRI-negative temporal lobe epilepsy. Epilepsia 50, 234-239.

LoPinto-Khoury, C., Sperling, M.R., Skidmore, C., Nei, M., Evans, J., Sharan, A., Mintzer, S., 2012. Surgical outcome in PET-positive, MRI-negative patients with temporal lobe epilepsy. Epilepsia 53, 342-348.

Minoshima, S., Berger, K.L., Lee, K.S., Mintun, M.A., 1992. An automated method for rotational correction and centering of three-dimensional functional brain images. Journal of nuclear medicine : official publication, Society of Nuclear Medicine 33, 1579-1585.

Minoshima, S., Frey, K.A., Koeppe, R.A., Foster, N.L., Kuhl, D.E., 1995. A diagnostic approach in Alzheimer's disease using three-dimensional stereotactic surface projections of fluorine-18-FDG PET. Journal of nuclear medicine : official publication, Society of Nuclear Medicine 36, 1238-1248.

Minoshima, S., Koeppe, R.A., Frey, K.A., Kuhl, D.E., 1994. Anatomic standardization: linear scaling and nonlinear warping of functional brain images. Journal of nuclear medicine : official publication, Society of Nuclear Medicine 35, 1528-1537.

Mizumura, S., Kumita, S., 2006. Stereotactic statistical imaging analysis of the brain using the easy Z-score imaging system for sharing a normal database. Radiation medicine 24, 545-552.

Najm, I.M., Naugle, R., Busch, R.M., Bingaman, W., Luders, H., 2006. Definition of the epileptogenic zone in a patient with non-lesional temporal lobe epilepsy arising from the dominant hemisphere. Epileptic disorders : international epilepsy journal with videotape 8 Suppl 2, S27-35.

Ohta, Y., Nariai, T., Ishii, K., Ishiwata, K., Mishina, M., Senda, M., Hirakawa, K., Ohno, K., 2008. Voxel- and ROI-based statistical analyses of PET parameters for guidance in the surgical treatment of intractable mesial temporal lobe epilepsy. Annals of nuclear medicine 22, 495-503.

Parker, F., Levesque, M.F., 1999. Presurgical contribution of quantitative stereotactic positron emission tomography in temporo limbic epilepsy. Surgical neurology 51, 202-210.

Rubin, E., Dhawan, V., Moeller, J.R., Takikawa, S., Labar, D.R., Schaul, N., Barr, W.B., Eidelberg, D., 1995. Cerebral metabolic topography in unilateral temporal lobe epilepsy. Neurology 45, 2212-2223.

Sakamoto, S., Takami, T., Tsuyuguchi, N., Morino, M., Ohata, K., Inoue, Y., Ide, W., Hashimoto, I., Kamada, H., Tanaka, H., Hara, M., 2009. Prediction of seizure outcome following epilepsy surgery: asymmetry of thalamic glucose metabolism and cerebral neural activity in temporal lobe epilepsy. Seizure 18, 1-6.

Semah, F., Baulac, M., Hasboun, D., Frouin, V., Mangin, J.F., Papageorgiou, S., Leroy-Willig, A., Philippon, J., Laplane, D., Samson, Y., 1995. Is interictal temporal hypometabolism related to mesial temporal sclerosis? A positron emission tomography/magnetic resonance imaging confrontation. Epilepsia 36, 447-456.

Shimizu, H., Suzuki, I., Ohta, Y., Ishijima, B., 1992. Mesial temporal subdural electrode as a substitute for depth electrode. Surgical neurology 38, 186-191.

Soma, T., Momose, T., Takahashi, M., Koyama, K., Kawai, K., Murase, K., Ohtomo, K., 2012. Usefulness of extent analysis for statistical parametric mapping with asymmetry

index using inter-ictal FGD-PET in mesial temporal lobe epilepsy. Annals of nuclear medicine 26, 319-326.

Takahashi, M., Soma, T., Kawai, K., Koyama, K., Ohtomo, K., Momose, T., 2012. Voxel-based comparison of preoperative FDG-PET between mesial temporal lobe epilepsy patients with and without postoperative seizure-free outcomes. Annals of nuclear medicine 26, 698-706.

Theodore, W.H., Sato, S., Kufta, C.V., Gaillard, W.D., Kelley, K., 1997. FDG-positron emission tomography and invasive EEG: seizure focus detection and surgical outcome. Epilepsia 38, 81-86.

Uijl, S.G., Leijten, F.S., Arends, J.B., Parra, J., van Huffelen, A.C., Moons, K.G., 2007. The added value of [18F]-fluoro-D-deoxyglucose positron emission tomography in screening for temporal lobe epilepsy surgery. Epilepsia 48, 2121-2129.

Vinton, A.B., Carne, R., Hicks, R.J., Desmond, P.M., Kilpatrick, C., Kaye, A.H., O'Brien, T.J., 2007. The extent of resection of FDG-PET hypometabolism relates to outcome of temporal lobectomy. Brain : a journal of neurology 130, 548-560.

Wieser, H.G., Blume, W.T., Fish, D., Goldensohn, E., Hufnagel, A., King, D., Sperling, M.R., Luders, H., Pedley, T.A., Commission on Neurosurgery of the International League Against, E., 2001. ILAE Commission Report. Proposal for a new classification of outcome with respect to epileptic seizures following epilepsy surgery. Epilepsia 42, 282-286.

Willmann, O., Wennberg, R., May, T., Woermann, F.G., Pohlmann-Eden, B., 2007. The contribution of 18F-FDG PET in preoperative epilepsy surgery evaluation for patients with temporal lobe epilepsy A meta-analysis. Seizure 16, 509-520.

Wong, C.H., Bleasel, A., Wen, L., Eberl, S., Byth, K., Fulham, M., Somerville, E., Mohamed, A., 2010. The topography and significance of extratemporal hypometabolism in refractory mesial temporal lobe epilepsy examined by FDG-PET. Epilepsia 51,

1365-1373.

Wong, C.H., Bleasel, A., Wen, L., Eberl, S., Byth, K., Fulham, M., Somerville, E., Mohamed, A., 2012. Relationship between preoperative hypometabolism and surgical outcome in neocortical epilepsy surgery. Epilepsia 53, 1333-1340.

Legend of table

Individual data including following factors are described on table.

Age: age when they underwent surgery.

Age of onset: age when the first seizure was detected.

Duration: the duration of seizure,

Past history: Particularly the history of febrile seizure (FS) was considered.

Seizure type: CPS means complex partial seizure, and SGTC represents secondary generalized tonic clonic seizure. The semiology of CPS indicated the origin from mesial temporal lobe.

HS on MRI: If the laterality of hippocampal sclerosis on MRI was not clear, we defined 'unknown'.

scalp EEG interictal or ictal: When the interictal or ictal epileptiform discharges were located in F7 to T3 or F8 to T4 on EEG electrodes, epileptiform discharges were regarded as AT (anterior temporal). When discharges were seen around T3 to T5 or T4 to T6, they were defined MT (middle temporal). The abbreviations of location are as follows: 'T' as temporal, 'F' as frontal, and 'Bi' as bilateral.

Surgical procedure: SAH as selective amygdalohippocampectomy and ATL as anterior temporal lobectomy.

Surgical outcome 1 year and 2 years after surgery are presented.

RHD: The values of RHD in each ROI were presented.

Legends of figures

Figure 1

MRI and FDG-PET findings with and without 3D-SSP in the patients with well-lateralized epileptic focus. In this case, atrophic mesial temporal structures on MRI-FLAIR imaging show hypometabolism on the FDG-PET with and without the 3D-SSP analyses.

Figure 2

Comparison of RHD between the good and poor surgical outcome groups. In the good surgical outcome group, the RHD ipsilateral to the surgical side was significantly higher than that of the contralateral side in all of the ROIs. On the other hand, the RHD was not significant in all of the ROI in the poor surgical outcome group (＊:$p<0.05$).

Figure 3

The ROC curve of the RHD ‘hippocampus and amygdala’ ROI. ROC curve of RHD of ‘Hippocampus & Amygdala’ was described and AUC was 0.755 with SE = 0.017 and 95% CI from 0.561 to 0.949. According to the ROC curve, the best cut-off value with maximum sensitivity (0.7) and minimum fall-out (0.3) was 0.22.

Figure 4

The comparison of RHD between the concordant and discordant patients. In the concordant patients, the RHD in the ipsilateral side was significantly higher than that of the contralateral side. The hippocampus and amygdala showed a much higher RHD of

over 0.5. In the discordant patients, the RHD in every ROI showed a less significant value of RHD.

Figure 5

The comparison of RHD between the good and poor surgical outcome groups in the discordant group. In the good surgical outcome group, athe RHD in the ‘hippocampus and amygdala’ was significantly higher than in that of poor surgical outcome group. On the other hand, in the patients with poor surgical outcomes there was no significant difference from the RHDs between the good and poor outcome groups (∗:$p<0.05$).

Figure

Figure 1. MRI and FDG-PET findings with and without 3D-SSP.

MRI

FDG-PET without 3D-SSP

FDG-PET with 3D-SSP

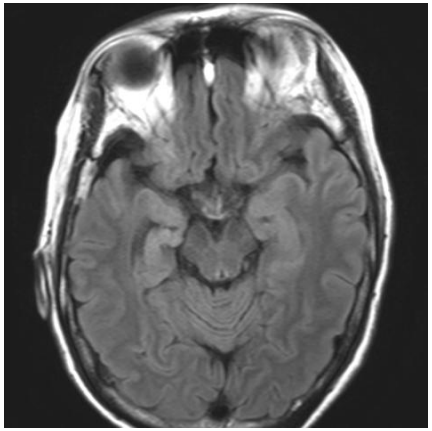

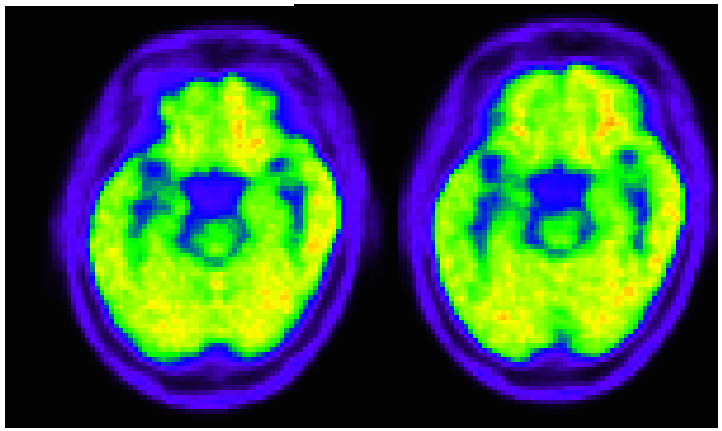

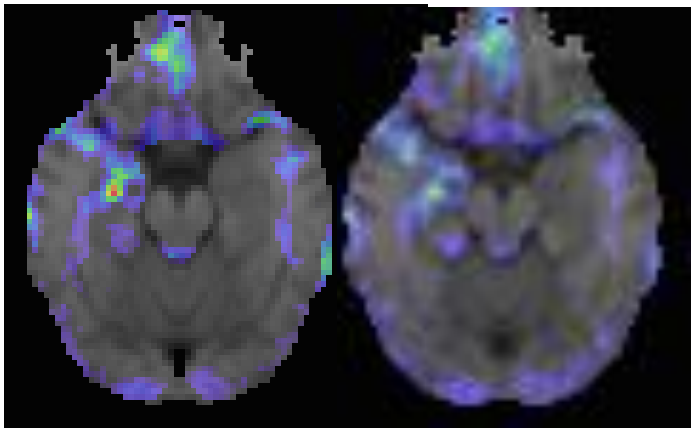

Figure 2. Comparisons of the RHDs according to surgical outcome in four ROIs.

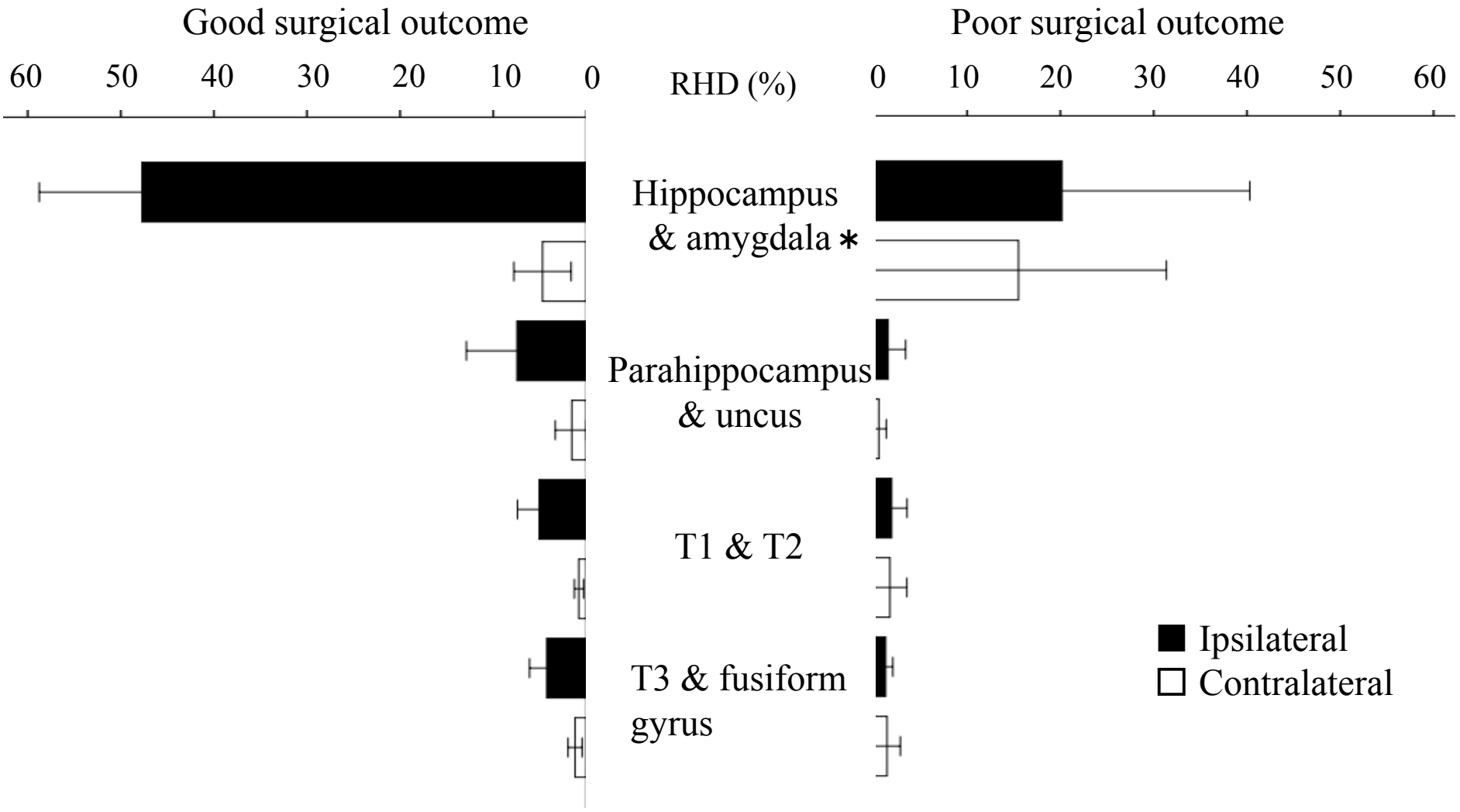

Figure 3. ROC curve for the RHD of the hippocampus and amygdala

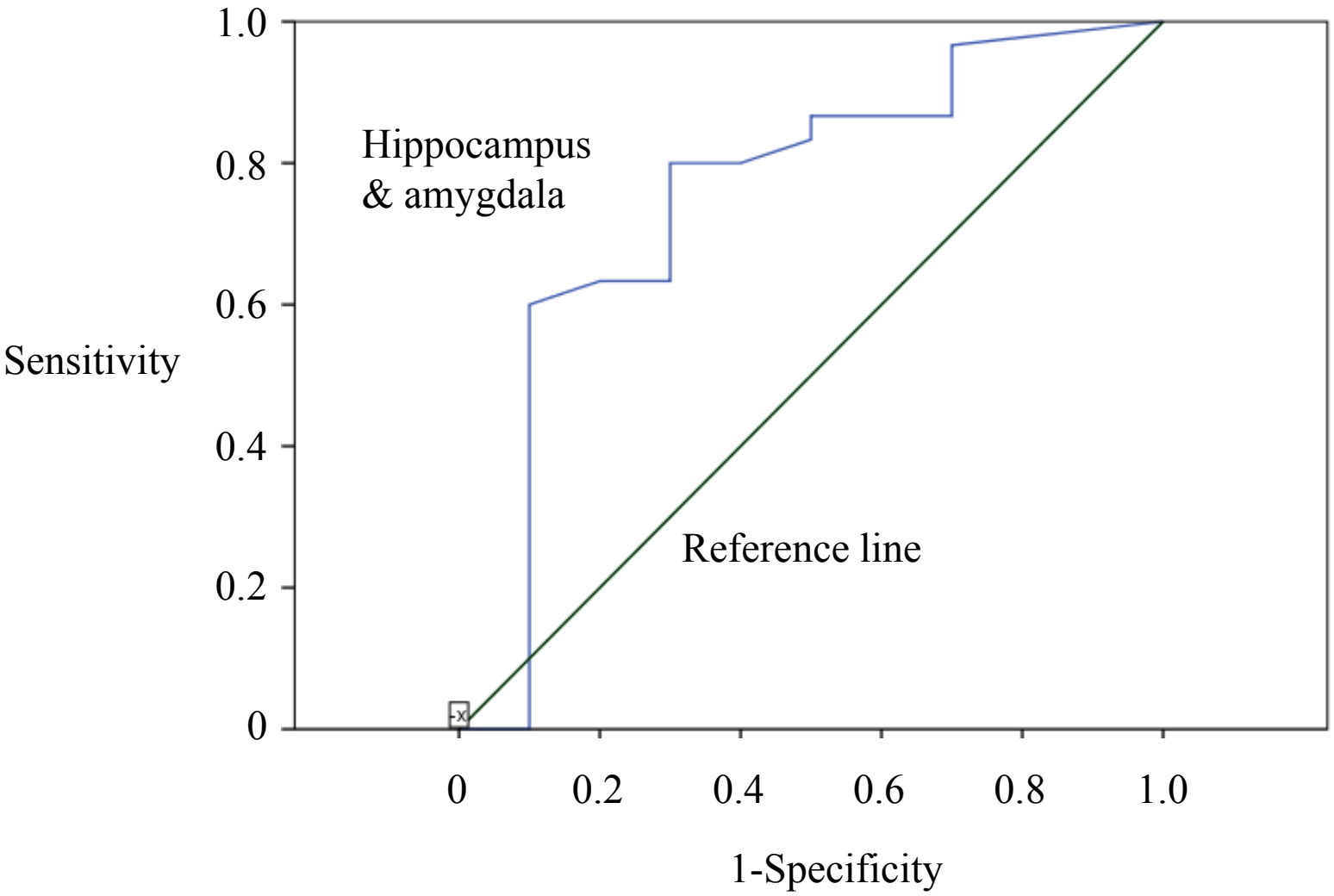

Figure 4. Comparisons of the RHD lateralities and presurgical non-invasive investigations according to concordance and discordance

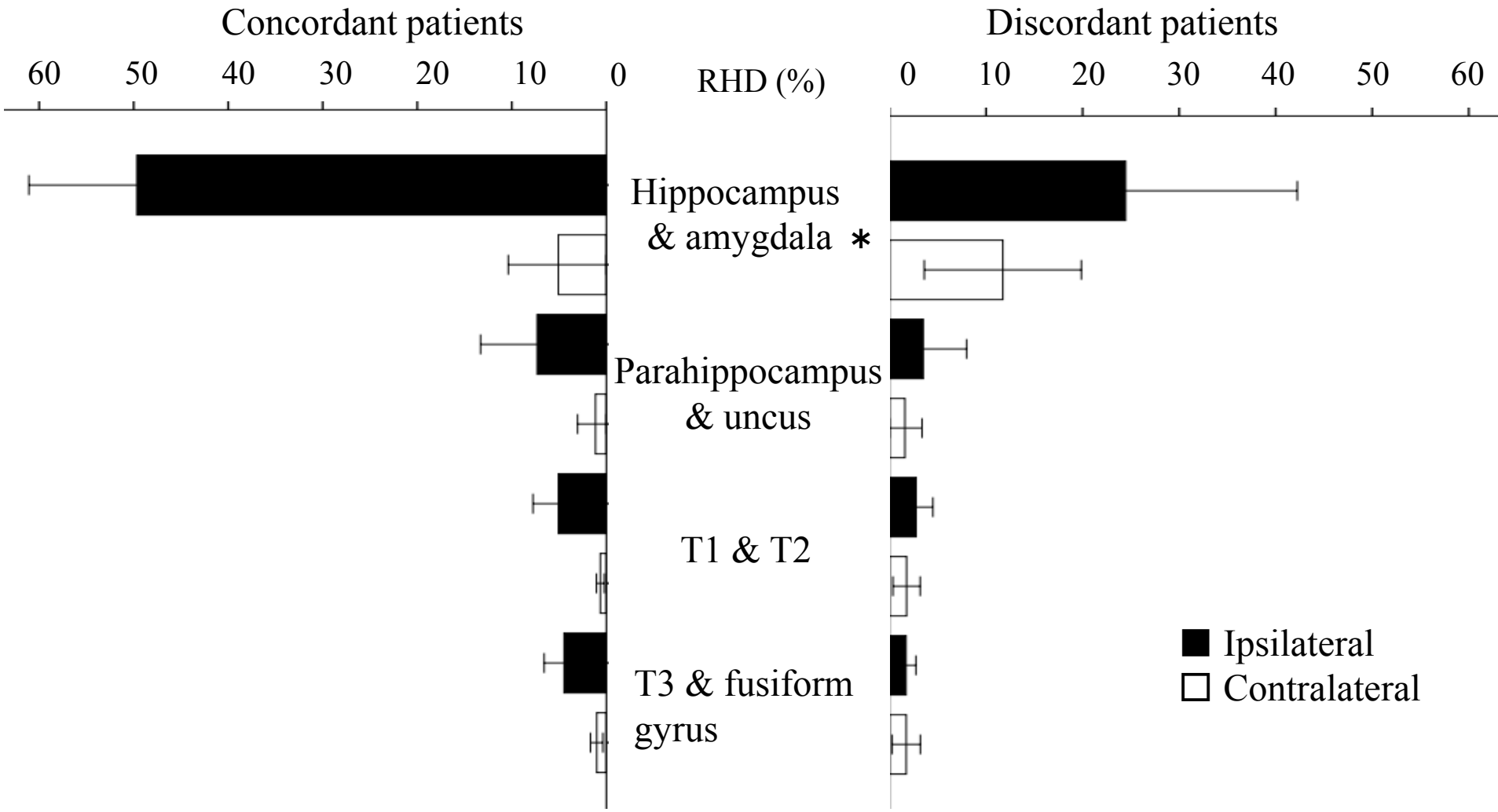

Figure 5. Comparison of the RHDs of discordant patients according to the presurgical evaluations

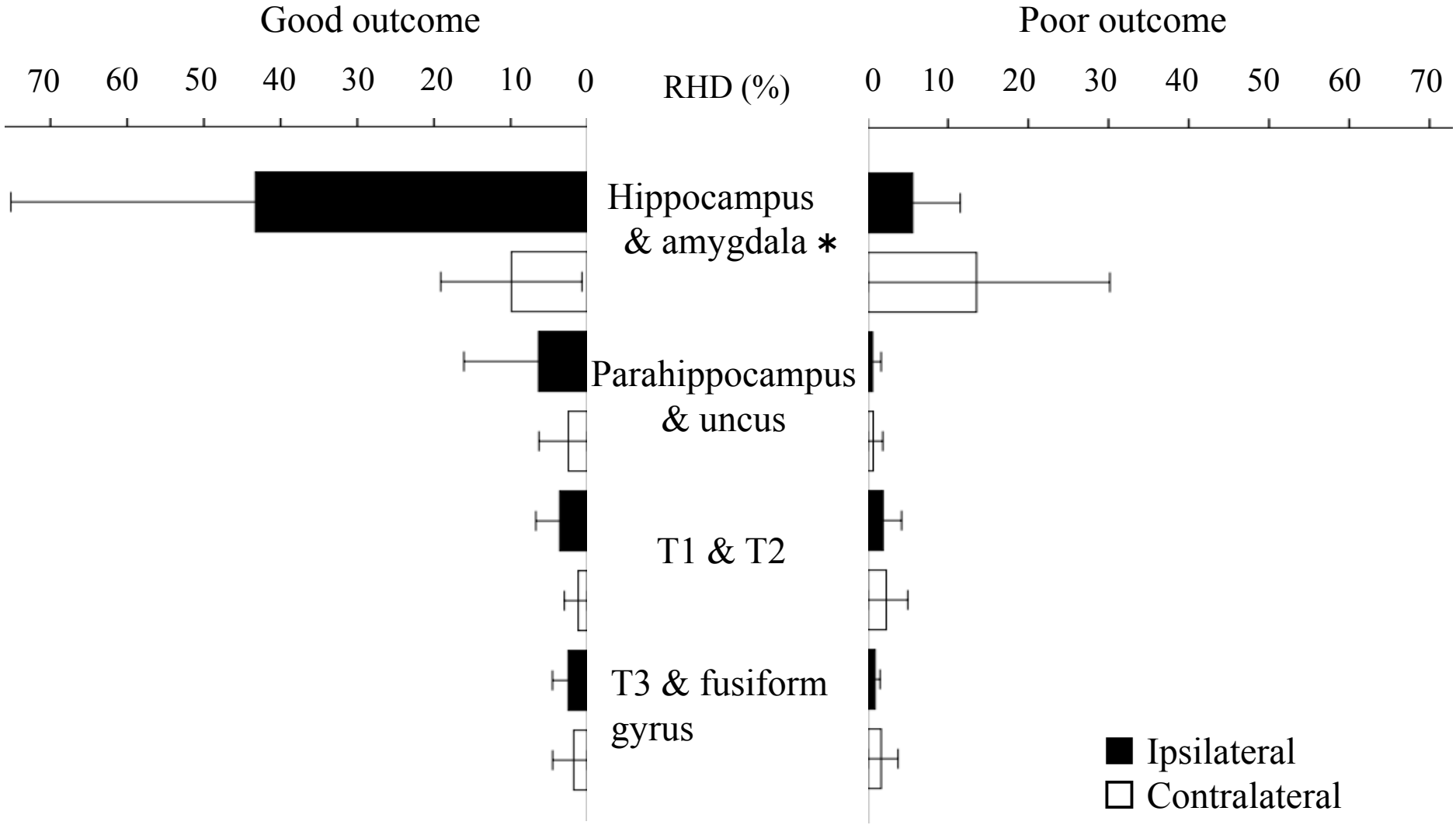

Supplementary Material

Click here to download Supplementary Material: HIGO supplementary table.xlsx